Monthly Notices
of the
ROYAL ASTRONOMICAL SOCIETY

MNRAS **531,** 1294–1307 (2024)
Advance Access publication 2024 April 27

https://doi.org/10.1093/mnras/stae1066

On the directional nature of celestial object's fall on the earth (Part 1: distribution of fireball shower, meteor fall, and crater on earth's surface)

Prithwish Ghosh,[1,2] Debashis Chatterjee [1]★ and Amlan Banerjee[3]

[1]*Department of Statistics, Siksha Bhavana (Institute of Science), Visva Bharati, Bolpur, Santiniketan 731235, India*
[2]*Department of Statistics, North Carolina State University, Raleigh, NC, 27607, USA*
[3]*Geological Studies Unit, Indian Statistical Institute, Kolkata, West Bengal 700108, India*

Accepted 2024 April 17. Received 2024 April 16; in original form 2023 August 31

ABSTRACT

This paper investigates the directional distribution of extraterrestrial objects (meteors, fireballs) impacting Earth's surface and forming craters. It also introduces a novel directional statistical mixture model to analyze their falls, validated through rigorous testing. First, we address whether these falls follow non-uniform directional patterns by explicitly employing directional statistical tools for analysing such data. Using projection techniques for longitude and latitude and more importantly, a general spherical statistical approach, we statistically investigate the suitability of the von Mises distribution and its spherical version, the von Mises–Fisher distribution, (a maximum entropy distribution for directional data). Moreover, leveraging extensive data sets encompassing meteor falls, fireball showers, and craters, we propose and validate a novel mixture von Mises–Fisher model for comprehensively analysing extraterrestrial object falls. Our study reveals distinct statistical characteristics across data sets: fireball falls exhibit non-uniformity, while meteor craters suggest a potential for both uniform and von Mises distributions with a preference for the latter after further refinement. Meteor landings deviate from a single-directional maximum entropic distribution; we demonstrate the effectiveness of an optimal 13-component mixture von Mises–Fisher distribution for accurate modelling. Similar analyses resulted in 3- and 6-component partitions for fireball and crater data sets. This research presents valuable insights into the spatial patterns and directional statistical distribution models governing extraterrestrial objects' fall on Earth, useful for various future works.

Key words: methods: data analysis – methods: statistical – meteorites, meteors, meteoroids.

1 INTRODUCTION

Meteoroids encompass a diverse array of celestial bodies, ranging from tiny dust particles to minor asteroids colloquially referred to as space rocks (Hochhaus & Schoebel 2015). When these meteoroids penetrate the Earth's or another planet's atmosphere at high speeds, they ignite, producing luminous fireballs commonly known as shooting stars or meteors (Grieve 1984). However, in rare instances, certain meteoroids survive the atmospheric descent and strike the ground, earning the designation of meteorites (Brown et al. 2002). Most meteoroids are small and burn up entirely in the atmosphere, never reaching the Earth's surface. However, more giant meteoroids, with sizes ranging from metres to kilometres, can survive their passage and impact the Earth's surface. Fireball showers occur when Earth passes through a comet's debris field. Comets are icy bodies that orbit the Sun and release dust and gas as they approach the Sun. This debris field consists of tiny particles of dust and rock, and when Earth intersects it, these particles enter the atmosphere at high speeds, creating multiple meteors visible from a specific region on Earth (Grieve & Shoemaker 1994). The impact of a giant meteorites releases tremendous energy, creating a crater at the impact site. The size and depth of the crater depend on the size and velocity of the impacting meteor (Grieve 1984). The phenomenon of meteoroids falling on Earth's surface is subject to complex interactions influenced by the planet's rotation and various environmental factors. This raises questions regarding the randomness of meteoroids fall distribution and the presence of specific underlying distributions, an area relatively unexplored in current literature.

1.1 Previous works

There is a plethora of literature addressing different facets of meteoroids descent and collisions. For instance, Fisher & Swanson (1968) analysed meteorite–earth collisions, identifying social factors influencing observations and challenging prior conclusions regarding anisotropy for different meteoroid classes. Dohnanyi (1970) explored collisional and radiative effects on meteoroid populations, supporting a cometary origin based on mass distribution and collision impact. Millard Jr & Brown (1963) studied meteorite falls, observing temporal patterns and suggesting reduced meteorite influx post-1940. Halliday & Griffin (1982) investigated meteorite fall rates, highlighting gravity and environmental influences. Ghosh (2023), an unpublished master's dissertation, proposed a novel spatiotemporal

★ E-mail: debashis.chatterjee@visva-bharati.ac.in

analysis linking meteorite falls to Earth's cycles and gravitational factors. Brown et al. (1996) documented the St-Robert meteorite shower, providing insight into the event's characteristics. Whillans & Cassidy (1983) modelled constant meteorite influx and steady glacial conditions near Allan Hills in Antarctic regions. Wetherill (1968) explored potential meteorite sources near Jupiter, such as Hilda, Trojan asteroids, or short-period comets. These studies collectively contribute to understanding meteorite phenomena and their implications for Earth's environment and history. A study by Jenniskens et al. (2021) presents the detection of 14 meteor showers and six likely associations with long-period comets, employing low-light video cameras, elucidating distinctive characteristics, and orbital parameter constraints. A comprehensive examination of the Yarkovsky effect encompasses its diurnal and seasonal variations, particularly emphasizing its relevance for meteorite-sized asteroid fragments, is presented in Farinella, Vokrouhlickỳ & Hartmann (1998). Ye, Brown & Pokornỳ (2016) provide a survey utilizing meteor orbit data that identifies five significant meteor showers, confirming a minimum threshold for dormant comet presence in the near-Earth object population and supporting disruption as the prevailing end state for Jupiter-family comets. Similar significant works on Meteor can be found in Kronk (1988), Bruno et al. (2006), Sturm et al. (2015), and Bowen (1956) where the study employs the nearest-neighbour methodology to quantify the spatial distribution of terrestrial volcanic rootless cones and ice mounds, revealing clustering tendencies indicative of their geological origins and applies the same methodology to Martian features, demonstrating consistency with both ice mound or rootless cone origins, but not impact craters, underscoring the potential of nearest-neighbour analysis for feature discrimination. Remote sensing and geophysical techniques successfully uncover new insights into the geological structure and formation mechanics of the Ries crater, including discovering previously unidentified mega block structures within its mega block zone (Robbins 2019). Analysis of a 400-yr historical catalogue of meteoroid falls unveils synchronization with solar barycentric parameters, highlighting Jupiter-associated periodicities and emphasizing the importance of understanding meteoroid falling patterns to anticipate potential impacts (Herrera & Cordero 2016). However, very little literature exists examining the statistical distribution of meteor falls on the Earth's surface. To our knowledge, the only previous literature on statistical properties of overall meteor fall on the Earth's surface we found is de la Fuente Marcos & de la Fuente Marcos (2015), where the authors statistically establish the non-randomness of the meteor fall distribution on the surface of the Earth by using various traditional statistical tests for randomness. Directional statistical analysis is preferred for studying the spatial distribution of meteors or celestial objects due to its consideration of the circular nature of directional data, such as azimuthal or angular measurements (Corcoran, Chhetri & Stimson 2009). Traditional statistical methods may lead to misinterpretation or biased outcomes when applied to circular data Jammalamadaka & SenGupta (2001), Mardia, Jupp & Mardia (2000), and Mardia & Jupp (2009). In angular distribution studies characterized by latitude and longitudes, events are often characterized by direction, making directional statistics a more suitable framework Mardia et al. (2000), Jammalamadaka & SenGupta (2001), and Kubiak & Jonas (2007).

1.2 Objective of this paper

This paper investigates the spatial directionality of extraterrestrial object impacts on Earth. We address two key objectives:

(1) Non-randomness: we determine if these impacts occur randomly or exhibit patterns, building upon prior work by de la Fuente Marcos & de la Fuente Marcos (2015) and employing directional statistics suited for analysing geographic coordinates.

(2) Directional model: We propose and validate a novel probabilistic model based on the von Mises–Fisher distribution to capture these directional patterns. This model serves as a foundation for future research. The first part of this paper addresses whether these falls occur randomly or exhibit specific patterns, an understudied area in the existing literature. Furthermore, The second part of this paper this research searches for a deeper understanding of extraterrestrial object falls and their spatial distribution on Earth by proposing a directional probabilistic model and statistically validating that using directional statistical von Mises–Fisher distribution, which maximizes entropy under certain assumptions. We propose and validate a novel stochastic model for extraterrestrial objects falling on the Earth's surface, which aims to serve as a theoretical starting point for relevant future investigations. de la Fuente Marcos & de la Fuente Marcos (2015) affirmed meteor fall non-randomness using traditional statistical methods, and we start from re-examining their claim while using directional statistical tools tailored for analysing angular data like geographic coordinates. Not only de la Fuente Marcos & de la Fuente Marcos (2015) not use directional statistical tools which should have been more suitable in this context, but their data set size was limited also: the B612 Foundation meteorite data set was employed, and only 33 data points were utilized in their paper, which may raise serious question on statistical confidence of testing the claimed hypothesis. In this paper, we overcome these limitations by utilizing three extensive data sets: the craters data set (72 data sets), the Fireball data set (960 data sets), and most importantly, the meteor landing data set (45 717 data points we have utilized in our paper). Conceivably, the meteor data set of de la Fuente Marcos & de la Fuente Marcos (2015) and this paper primarily was collected meteor data from land-based observations. To address this possible limitation, we incorporated three data sets. One data set includes fireball observations spanning the entire world map. The second data set encompasses crater formations caused by meteors, and the third data set covers meteor landings. We extend the work of de la Fuente Marcos & de la Fuente Marcos (2015) by leveraging extensive data sets to reveal nuanced distribution patterns beyond localized concentrations. More importantly, in the second part of this paper, we propose and validate a novel mixture of the von Mises–Fisher type probabilistic mixture model incorporating extensive data including meteor falls, fireball showers, and craters, which is the main novel objective of this paper. Our study focuses on the directional characteristics of extraterrestrial objects that fall on Earth's non-flat surface. We employ projection techniques for converting geographic coordinates and direct spherical distribution assessment. We also explore the suitability of the von Mises distribution and its spherical counterpart, the von Mises–Fisher distribution. These are maximum entropic distributions and are particularly suited for analysing directional data entropy maximization under certain constraints. Additionally, we emphasize the importance of simultaneously considering longitude and latitude for comprehensive pattern evaluation, utilizing spherical statistics for enhanced statistical precision. We identified distinct distribution patterns across the data sets. Fireball data displayed a non-uniform distribution, indicating they do not fall randomly. Meteor crater data hinted at a combination of random and directional (von Mises) distributions, with further analysis favouring the mixture von Mises–Fisher model. Meteor landing data exhibited the most complex pattern, requiring an optimum of 13-component von Mises–Fisher mixture model for accurate representation on the sphere.

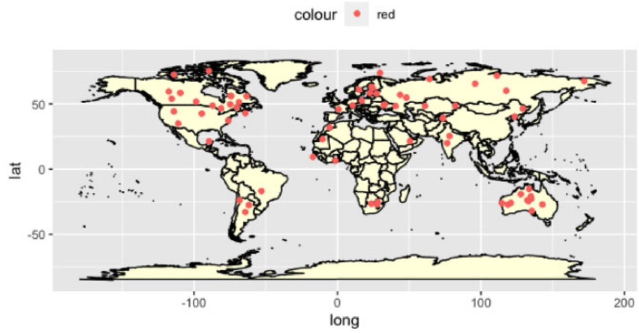

Figure 1. Crater created after the impact: first data set.

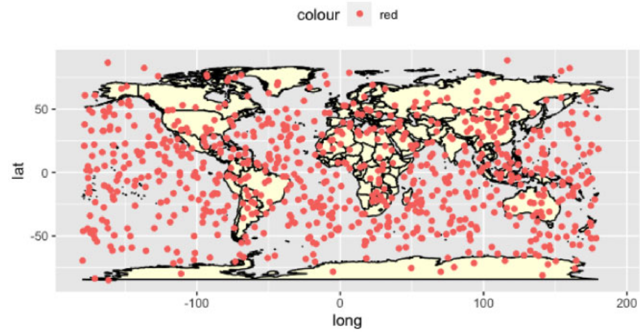

Figure 2. Fireball strikes on Earth (second data).

Fireball and crater data needed simpler models with optimal 3 and 6 components, respectively.

2 ABOUT THE METEOR CRATER DATA SETS, FIREBALL FALL, AND METEOR LANDING DATA SETS

We have taken data sets of extraterrestrial objects that fall on the surface of the Earth. The craters data set (72 data sets), the Fireball data set (960 data sets), and most importantly, the meteor landing data set (45 717 data points we have utilized in our paper). Among them, only one of our data sets (meteor fall) is similar, as considered in de la Fuente Marcos & de la Fuente Marcos (2015) for which 45 717 data points we have utilized in our paper, in contrast to the limited number of data sets of de la Fuente Marcos & de la Fuente Marcos (2015).

We used the first data set from https://web.archive.org/web/20130708142632/, http://www.passc.net/EarthImpactDatabase/index.html, where the data sets are from different periods. This data set gives us the location of the craters created by the meteors which fell on Earth. For a visual representation of the data, please refer to Fig. 1. This graphical depiction offers insights into how the craters are created by the meteor strike on our planet.

The data set used in the research article de la Fuente Marcos & de la Fuente Marcos (2015) is collected from the B612 project, which tells us the location of meteor strikes on Earth. However, as per the Supporting Information, the data set is said to be controversial http://www.passc.net/EarthImpactDatabase/index.html and https://web.archive.org/web/20130708142632/ .

The second data set gives essential details concerning each reported fireball event, encompassing the date and time of occurrence, the approximate total optical radiated energy, and the calculated total impact energy. Additionally, the data table includes information about the event's geographic location, altitude, and velocity at peak brightness, which we intends for future works. In astronomical terms, a fireball is an unusually bright meteor that reaches a visual magnitude of -3 or brighter when seen at the observer's zenith. The objects responsible for fireball events can be larger than one meter. When these fireballs explode within the Earth's atmosphere, they are technically termed 'bolides', although the terms fireballs and bolides are often used interchangeably in everyday language. The data set is collected from https://cneos.jpl.nasa.gov/fireballs/.

For a graphical depiction of the data, please refer to Fig. 2. This visual representation offers insights into the characteristics and distribution of fireball events, helping to elucidate their nature and impact energy.

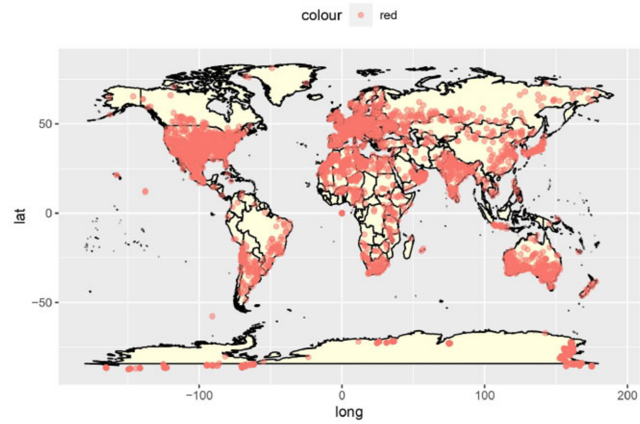

Figure 3. Meteor landing on Earth plotted on the world map.

We collected the meteorite fall data set from https://data.nasa.gov/Space-Science/Meteorite-Landings/gh4g-9sfh. Here, the Meteoritical Society collects data on meteorites that have fallen to Earth from outer space. This data set includes the location, mass, composition, and fall year for over 45 000 meteorites that have struck our planet. This data set has many parameters but used 'reclat' and 'reclong' as primary parameters. Note that a few column names start with 'rec' (e.g. recclass, reclat, and reclon). According to The Meteoritical Society, these are the recommended values of these variables. In some cases, there were historical reclassifications of a meteorite or small changes in the data on where it was recovered; this data set gives the currently recommended values. The visualization of the data set is given in Fig. 3.

Most meteorites are discovered in Antarctica due to a combination of factors. While the latitudes around 45° north and south of the equator generally experience more meteorite falls due to the Earth's axial tilt, the prevalence of meteorites in Antarctica is primarily attributed to its unique characteristics (Tollenaar et al. 2022). The contrast between dark meteorites and the white glacier landscape makes them easier to spot, contributing to a higher discovery rate. Additionally, Antarctica's isolation and minimal human activity help preserve meteorites, making it an ideal environment for their collection and study (Zekollari et al. 2019). Nonetheless, meteorites are abundantly found in Antarctica because it is relatively easy to spot a dark rock against the backdrop of a white glacier. This phenomenon is unique to Antarctica and is a prime location for meteorite discoveries. Scientists have plucked more than 45 000 meteorites from the ice in Antarctica https://earthobservatory.nasa.gov/images/149554/finding-meteorite-hotspots-in-antarctica. In our

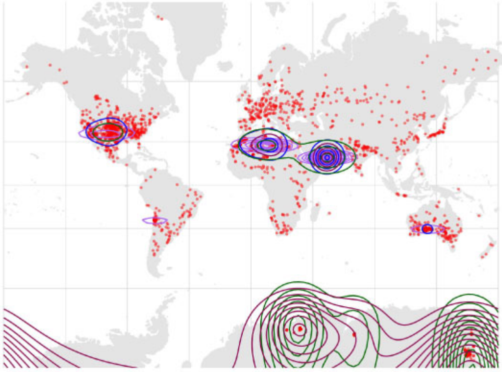

Figure 4. Spherical density estimate of meteor landing data set on Earth. We used the von Mises–Fisher's kernel contour plot for this data set. For the 2D picture, we plotted this. In this picture, we used the line spacing to denote the density, and the other line defines the more prominent contour. Most meteorites are discovered in Antarctica due to a combination of factors. The contrast between dark meteorites and the white glacier landscape makes them easier to spot, contributing to a higher discovery rate. Additionally, Antarctica's isolation and minimal human activity help preserve meteorites, making it an ideal environment for their collection and study. In the above plot, we plotted the density and contour plot with dark pink and dark colours for the Antarctica region. The other plots are as it is with the and concerning the non-Antarctica region.

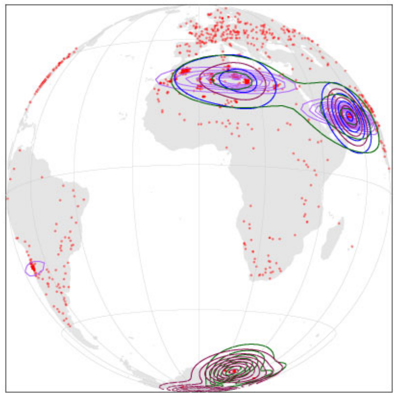

Figure 5. Spherical orthographic projection density for meteor landing data set. In this picture, we used the line spacing to denote the density, and the line defines the more prominent contour. Most meteorites are discovered in Antarctica due to a combination of factors. The contrast between dark meteorites and the white glacier landscape makes them easier to spot, contributing to a higher discovery rate. Additionally, Antarctica's isolation and minimal human activity help preserve meteorites, making it an ideal environment for their collection and study. In the above plot, we plotted the density and contour plot with dark pink and dark colours for the Antarctica region. The other plots are as it is with and concerning the non-Antarctica region.

meteor landing data set, we get that nearly 20000 + data set for meteor landing is placed the Antarctica Region. We plotted the data set density and contour plot in Figs 4 and 5. Our investigations reveal that the distribution of meteorite strikes does not demonstrate uniformity, the same conclusion made in de la Fuente Marcos & de la Fuente Marcos (2015). Moreover, We aim to derive a distributional outcome for meteorite impacts. Given that the striking locations span the entire globe, we analyse the data using circular or directional statistics, which are well suited for analysing such geographically dispersed events. We conclude that almost all meteor crater and fireball data set's latitude and longitude projections follow von Mises, the 'most entropic' circular distribution under a given first moment.

2.1 Assumptions related to maximum entropic phenomena

We state two assumptions about extra-terrestrial objects falling on Earth's surface.

ASSUMPTION 1: METEOR CRATER, FIREBALL FALL, METEOR LANDING, AND SIMILAR EXTRATERRESTRIAL OBJECTS FALLING ON THE EARTH'S SURFACE ARE SPATIAL STOCHASTIC PROCESSES.

ASSUMPTION 2: METEOR CRATER, FIREBALL FALL, METEOR LANDING, AND SIMILAR EXTRATERRESTRIAL OBJECTS FALLING ON THE EARTH'S SURFACE ARE 'MAXIMUM ENTROPIC SPATIAL PROCESSES.'

It is to be noted that, although not explicitly mentioned, de la Fuente Marcos & de la Fuente Marcos (2015) actually have taken the Assumption 1. The maximum entropy principle states that given constraints, a system tends towards the state with the highest possible entropy (Ash 2012). Entropy, in this context, is a statistical measure of a system's disorder or randomness. The von Mises distribution is the 'maximum entropy distribution' that is specific to a constrained scenario on the mean direction and the concentration parameter (Mardia et al. 2000; Jammalamadaka & SenGupta 2001; Mardia & Jupp 2009). These constraints restrict the possible distribution shapes (Jupp 1995; Mardia et al. 2000). In other situations, such as unconstrained scenarios, different distributions, such as uniform distribution, might be more appropriate depending on the available information and the intended analysis. From theoretical statistical intuition and previous literature like Millard Jr (1963), Millard Jr & Brown (1963), Fisher & Swanson (1968), Wetherill (1968), Dohnanyi (1970), Halliday & Griffin (1982), Whillans & Cassidy (1983), Brown et al. (1996), and Ghosh & Chatterjee (2023) which have examined various aspects of meteorite falls and collisions, Assumptions 1 and 2 comes from the hypothesis that meteor falls and similar extraterrestrial objects falling on the Earth's surface could be hypothetically a 'maximum entropic process.'

This opinion on the first moment being broadly specified can be intuitively ascertained from the observation that the relative positions of the Earth from the moving meteor belt around the sun are deterministic (in the sense that there is no overwhelmingly unpredictable randomness arising from relative motion). Moreover, consider the overall deterministic nature of the Earth's rotation and its Milankovitch cycle, all of which affects the overall distribution pattern of extraterrestrial object fall. We may need to partition the Earth's surface to account for continental clusters due to missing data into the ocean. Not so surprisingly, spherical uniforms are not the maximum entropic distribution under specified first-moment conditions. Instead, the von Mises distribution is the maximum entropy distribution for directional data (when the first circular moment is specified). Hence, based on statistical intuition, von Mises or similar maximum entropic distribution are suitable candidates, alongside directional uniform distribution, for further statistical investigations on whether they fit well.

3 DIRECTIONAL STATISTICAL PRELIMINARIES

3.1 Directional statistical preliminaries

We start with essential definitions and properties of certain directional statistical distributions and directional statistical tests. For more detailed information, we refer to Jammalamadaka & SenGupta (2001).

3.2 von Mises distribution

The von Mises distribution is a probability distribution that models circular data, such as directions around a circle (e.g. compass angles and wind directions; Jammalamadaka & SenGupta 2001). Under moment constraints, the von Mises distribution maximizes the entropy compared to other probability distributions capable of representing circular data (Mardia et al. 2000; Jammalamadaka & SenGupta (2001). Given the specified constraints, it reflects the state of the highest possible disorder given the specified constraints. It allows for characterizing the distribution of observations with a preferred direction and a certain level of dispersion around that direction. A circular random variable θ follows the von Mises distribution (also known as the circular normal distribution and a close approximation to the wrapped normal distribution) and is characterized by the probability density function (pdf; Mardia 1972)

$$f(\theta;\mu,k)=\frac{1}{2\pi I_0(k)}e^{k\cos\theta(\theta-\mu)}. \tag{1}$$

In this equation, θ lies in the range $[0, 2\pi)$, μ is constrained to $[0, 2\pi)$, and $(k > 0)$. The normalizing constant $I_0(k)$ is the modified Bessel function of the first kind and order zero, given by:

$$\frac{1}{2\pi}\int_1^{2\pi}\exp(k\cos\theta)\mathrm{d}\theta=\sum_{r=0}^{\infty}\left(\frac{k}{2}\right)^{2r}\left(\frac{1}{r!}\right)^2. \tag{2}$$

To determine the cumulative distribution of the circular normal or the von Mises distribution, we integrate the pdf, resulting in the following cumulative distribution function (cdf):

$$F(\theta)=\frac{1}{2\pi I_0(k)}\left(\theta I_0(k)+2\sum_{p=1}^{\infty}\frac{I_p(k)\sin p(\theta-\mu)}{p}\right), \tag{3}$$

where θ is confined to the interval $[0, 2\pi)$.

We utilize the von Mises distribution to perform distribution checking on the given data, which provides insights into meteor shower patterns around the world.

3.3 von Mises–Fisher distribution

The von Mises–Fisher distribution VMF($\boldsymbol{\mu}, \kappa$) is the natural extension of the von Mises distribution on the unit circle to the hypersphere of higher dimensions (sphere in our case). It is an important isotropic distribution for directional data and statistics. The von Mises–Fisher distribution is a distribution on the surface of a sphere. It has two parameters: the mean direction and the concentration (analogous to a normal distribution's mean and standard deviation). Its distribution, in terms of the point $\boldsymbol{x} = \{x_1, x_2, x_3\}$ on a circle of unit length is

$$f(\boldsymbol{x};\boldsymbol{\mu},\kappa)=C_3(\kappa)\exp\left(\kappa\boldsymbol{x}\cdot\boldsymbol{\mu}\right). \tag{4}$$

Here, κ is the concentration, μ (a unit vector) is the mean direction, $\boldsymbol{x}$ is the random unit vector, and $C_3(\kappa)$ is the normalization coefficient, which can be shown to be dependent only on κ and the dimension (3, in case of the sphere). For details, we refer to Mardia et al. (2000) and Watson (1982).

3.4 Wrapped uniform distribution

If we do not have any prior information about the mean direction or concentration (unconstrained scenario), then the uniform distribution on the circle maximizes the entropy. This is because the uniform distribution allows for complete randomness in all directions, representing the most disordered state. In the wrapped uniform distribution, the total probability is uniformly spread out along the circumference of a circle. When $\kappa = 0$, the von Mises–Fisher distribution VMF($\boldsymbol{\mu}, \kappa$) on sphere surface S^{p-1} ($p = 3$) simplifies to the uniform distribution on $S^{p-1} \subset \mathbb{R}^p$. The density is constant with the value $C_p(0)$. The circular version of uniform distribution characterized by a constant density given by Mardia (1972):

$$f(\theta)=\frac{1}{2\pi}. \tag{5}$$

All directions on the circle are equally likely in this distribution, leading to its alternative names, such as the isotropic or random distribution.

3.5 Watson test

In this study, we primarily employed Watson-type tests to examine whether the positional data adhere to either a von Mises distribution or a Circular Uniform Distribution.

Wheeler & Watson (1964) introduced a statistic for directional data, similar to the Kolmogorov–Smirnov non-parametric test, to assess the goodness of fit of one-sample and two-sample data concerning the uniform distribution or von Mises distribution. Watson's statistic is defined as follows:

$${W_n}^2=\int_0^{2\pi}\left[(F_n-F)-\int_0^{2\pi}(F_n-F)\,\mathrm{d}F\right]^2\mathrm{d}F, \tag{6}$$

where W_n represents Watson's statistic, $F_n(\alpha)$ denotes the empirical distribution function, which is based on the ordered observations $\alpha_{(1)} \leqslant \cdots \leqslant \alpha_{(n)}$ of a sample of independent and identically distributed variables $\alpha_1, \alpha_2, \cdots, \alpha_n$ drawn from the distribution $F(\alpha)$. F represents the actual distribution function, that is,$F = F_0(\alpha)$. An alternative representation of Watson's statistic is given by:

$${W_n}^2=\sum_{i=1}^{n}\left[\left(U_{(i)}-\frac{i-\frac{1}{2}}{n}\right)-\bar{U}-\frac{1}{2}\right]^2+\frac{1}{12n}. \tag{7}$$

Here, $U_i = F(\alpha_i)$, and the Cramer–von Mises statistic can be viewed as the 'second moment' of $(F_n - F)$. Watson's statistic resembles the expression for 'variance' in certain aspects.

Using Watson tests, we can examine whether the given positional data aligns with the expected distributions, aiding our analysis of the underlying patterns in the data.

3.6 Rao spacing test

The Rao spacing test is the test for determining the uniformity of the data. It uses the space between observations to determine if the data show significant directionality. The test statistic U for Rao's spacing test is defined by:

$$U=\frac{1}{2}\sum_{i=1}^{n}|T_i-\lambda|, \tag{8}$$

where

$$\lambda=\frac{360}{n},\,T_i=f_{i+1}-f_i,\,T_n=(360-f_n)+f_1.$$

The test statistic aggregates the deviations between consecutive points, each weighted by the total number of observations in the data set. Rao's Spacing test determined the data to show no signs of directional trends. We cannot reject the null hypothesis of uniformity and will assume uniformity concerning the direction of arrival.

4 INITIAL INFERENCES FROM CIRCULAR PP PLOT

P–P plot (probability–probability plot or per cent– per cent plot or P value plot) is a probability plot for assessing how closely two data sets agree or how closely a data set fits a particular model. It works by plotting the two cdfs against each other; the data will appear nearly a straight line if they are similar. Technically, A P–P plot plots two cdfs against each other: given two probability distributions, with cdfs F and G, it plots $(F(t), G(t))$ as t ranges from $-\infty$ to ∞. This behaviour is similar to the more widely used Q–Q plot. The P–P plot is only helpful for comparing probability distributions with nearby or comparable locations. It will pass through the point $(1/2, 1/2)$ if and only if the two distributions have the same median.

For instance, the von Mises probability–probability plot plots the empirical distribution of a data set against the best-fitting von Mises distribution function. The maximum-likelihood estimates of the parameters of the von Mises distribution are calculated from the given data set. The empirical distribution function is plotted against a von Mises distribution function. Similarly, uniform circular probability–probability plots the empirical distribution of a data set against a uniform circular distribution function.

We plotted the probability–probability plot for all the data sets for both location parameters concerning the circular distribution, von Mises, and circular uniform distribution. The pictures of the P–P plot are mentioned in the Section 1.1 (Appendix A). This method is used because the lack of data points of location parameters in the crater data set satisfies the Watson test for both circular distributions (von Mises and circular uniform). To get a distribution that fits better with that data set, we used the PP plot and compared it between von Mises and circular uniform. We also tested or plotted this pp plot for all three data sets to visualize all the data set location parameters.

5 STATISTICAL RESULTS

Circular data analysis tools are used to analyse the nature of meteor strike locations, where data ares inherently cyclical or angular. In scenarios like meteor impacts, the locations are often measured in degrees around a circular scale, like the Earth's surface. Traditional linear statistical methods can lead to erroneous interpretations and biased estimates due to the periodic nature of circular data. By adopting circular data analysis, we can accurately model and interpret the patterns and trends in meteor impact locations. This leads to more informed conclusions and a better understanding of the underlying processes driving these occurrences.

We cannot reject the null hypothesis from the tables if the critical value exceeds the test statistics for a given significance level (0.05). Where the null hypothesis is, the data follows a von Mises distribution. Similarly, for the circular uniform distribution, the test conducts the same null hypothesis testing concerning their critical value and test statistics.

We also tested the Watson two-sample test to see if the distribution of the two samples was equal. The null hypothesis is the two distributions are similar.

Table 1. Homogeneity test for two circular samples of fireball satisfy that the meteor or fireball parameters which are longitude and latitude satisfied for von Mises distribution.

Data set name	Critical value	α-value	Test statistics
Fireball data	0.187	0.05	0.0588

Table 2. Watson test result for data set 2 for 0.05 significance level showed us that the data set will follow a circular distribution if it does not reject the null hypothesis. Here, the null hypothesis is that the critical value is more than the test, which is not satisfied accordingly.

Parameter	Test statistics	Critical value	Distribution
Longitude	0.0283	0.061	von Mises distribution
Latitude	0.0293	0.061	von Mises distribution

Table 3. Rao spacing test result for fireball data for 0.05 level of Significance showed us that the data set will follow a circular distribution if it does not reject the null hypothesis. Here, the null hypothesis acceptance requires that the critical value exceeds the test statistic, which is not satisfied accordingly.

Parameter	Test statistic	Critical value	Distribution
Longitude	156.05	137.46	Not circular uniform
Latitude	194.0331	137.46	Not circular uniform

Table 4. Watson test result for data set of craters created by meteors for 0.05 level of significance both of the data set follows a von Mises distribution.

Parameter	Test statistics	Critical value	Distribution
Longitude	0.0588	0.061	von Mises distribution
Latitude	0.0269	0.061	von Mises distribution

5.1 Results on distributions of fireball fall on the Earth

5.1.1 Directional statistical test for homogeneity of fireball fall on the Earth

The test for homogeneity of the fireball data set location parameter result is summarized in Table 1.

5.1.2 Directional statistical test of whether fireball fall on the Earth follows von Mises distribution

We pursued to assess whether the data adhere to a von Mises distribution. We used the Watson and Rao spacing tests for the location parameters. The summary of the two tests is given in Tables 2 and 3.

5.2 Results on distributions of meteor crater on the Earth

5.2.1 Test of whether Crater's data on the Earth follows von Mises distribution

Similarly, we used the Watson and Rao spacing tests for the crater data set to check if the data set follows any circular distribution. Summary of the tests are given in Tables 4 and 5.

Table 5. Rao spacing test result for crater data for 0.05 level of significance showed us that the data set will follow a circular distribution if it does not reject the null hypothesis. Here, the null hypothesis is that the critical value is more than the test, which is not satisfied accordingly.

Parameter	Test statistics	Critical value	Distribution
Longitude	139.1891	148.34	Circular uniform
Latitude	134.7677	148.334	Circular uniform

Table 6. Homogeneity test for two circular samples of the crater, which tells us that both parameters satisfy the condition (test statistics are lower than the critical value) and are equal. Which satisfied the homogeneity between those two parameters.

Data set name	Critical value	α value	Test statistics
Crater value	0.187	0.05	0.0607

Table 7. Watson Test result for data set of meteor landing data set for 0.01 level of significance both of location parameters of the data set does not follow a von Mises distribution.

Parameter	Test statistics	Critical value
Longitude	135.2895	0.09
Latitude	90.735	0.09

Table 8. Watson test for uniformity check result for data set of meteor landing data set for 0.01 level of significance both of location parameters of the data set does not follow a circular uniform distribution.

Parameter	Test statistics	Critical value
Longitude	314.6936	0.267
Latitude	126.5393	0.267

5.2.2 Test for homogeneity of meteor crater on the Earth

The test for homogeneity of the crater data set location parameter result is summarized in Table 6.

REMARK 1. Tables 2 and 4 show that both location parameters follow von Mises distribution. But, till now, we cannot bypass the theory that the random nature of meteor falls. We need more tests of homogeneity to prove/disprove the random nature.

5.3 Results on distributions of meteor landing on the Earth

In the above two tests, we used the Watson test to test if the data set follows von Mises or circular uniform distribution. Tables 7 and 8 show that the meteor landing data set does not follow any circular distributions. The pictorial way is also given in Fig. 6 for the latitude parameter and the longitude location parameter.

5.3.1 Test of homogeneity for meteor landing data set

From Table 9, we get that the location parameters (longitude and latitude) for Meteor landing are not from the same distribution. Here, we used the Watson two test to get the results. The null hypothesis states that the distributions are the same for both parameters and are not the same as those used in the alternative hypothesis.

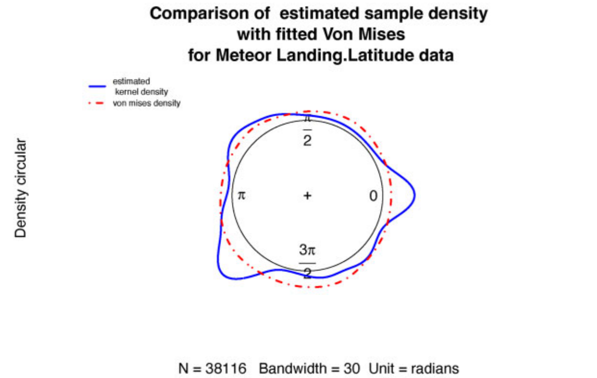

(a) This Figure consists of the Density plot of the latitude and the Von Mises distribution. Where the Blue color is the estimated kernel density and the dotted red line gives the Von Mises Density

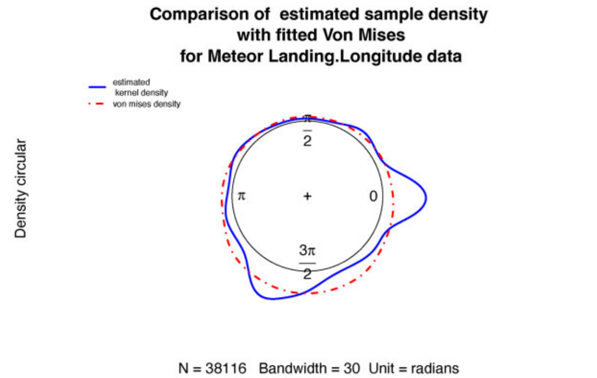

(b) This figure consists of the Density plot of the Longitude and the Von Mises Distribution over a unit circle. Where the Blue color is the estimated kernel density and the dotted red line gives the Von Mises Density

Figure 6. Plotted both density, generated from the mean direction, and κ value of the latitude parameter and overlapped to compare them. This will help us to infer more about the data set concerning the von Mises density function.

5.4 Distributional outputs for all of the data sets

The graphical representation of longitude and latitude on a unit circle is given in Figs 7(a) and (b), which are for the fireball data and in Figs 8(a) and (b) for the craters and the meteor landing data set the density plots are given in Figs 6(a) and (b). In these figures, the blue line denotes the kernel density of the location parameter (longitude or latitude), and then we compare those parameters with the red dashed line representing the density of von Mises where we took 1000 samples randomly from von Mises distribution concerning the circular mean and kappa values of the parameter.

In Tables 1, 6, and 9, we tested the homogeneity between the two location parameters (longitude and latitude) for both of the data sets (fireball and crater data sets). The test rejected the null hypothesis, which tells us that both data sets might follow spherical distribution for both data sets. But for the meteor landing data set, the homogeneity Table 9, we get that this is rejecting the null hypothesis,

Table 9. Test of homogeneity to determine whether the location parameters follow the same distribution.

Test statistics	Critical value	Output of null hypothesis
274.8671	0.268	Reject null hypothesis

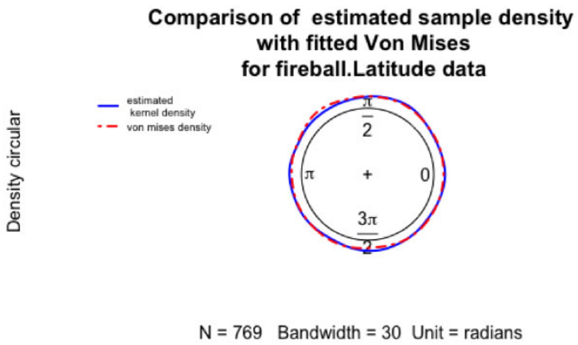

(a) Circular Density Plot of latitude for Fireball dataset

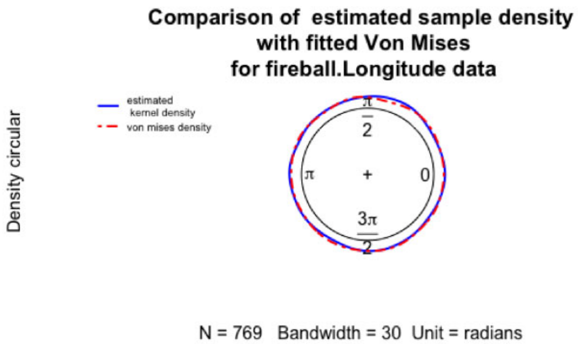

(b) Circular Density Plot of longitude for Fireball dataset

Figure 7. Circular density plot of latitudes and longitudes for fireball data set.

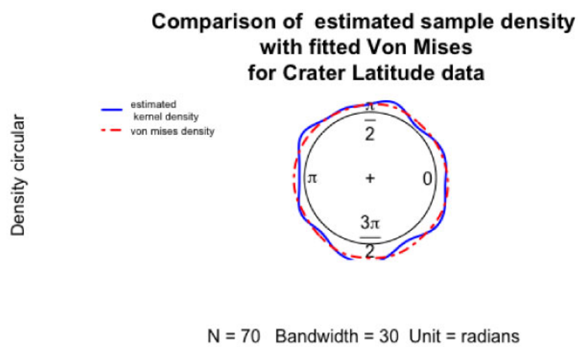

(a) Latitude plot for crater

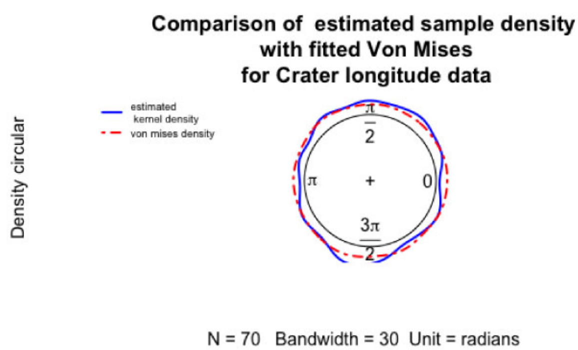

(b) Longitude plot for crater

Figure 8. Circular density plot of latitudes and longitudes for crater data set.

Table 10. Hypothesis test for von Mises–Fisher distribution over Kent distribution for crater data set where the *p*-value is 0.542 and the null hypothesis is whether a von Mises–Fisher distribution fits the data well, where the alternative is that Kent distribution is more suitable.

Test	Bootstrap *p*-value
9.184275	0.542000

Table 11. Hypothesis test for von Mises–Fisher distribution over Kent distribution for fireball data set where the *p*-value is 0.464 and the null hypothesis is whether a von Mises–Fisher distribution fits the data well, where the alternative is that Kent distribution is more suitable.

Test	Bootstrap *p*-value
5.64043	0.46400

which gives an output that the distribution of both location parameters is not from the same distribution, which is leaving the assumption of spherical distribution.

6 A COMPARISON BETWEEN KENT DISTRIBUTION AND VON MISES DISTRIBUTION

In this section, we used the limiting null distribution of Kent's statistic to test whether a sample comes from the Fisher distribution when *K*, the concentration parameter, goes to inf. A modification is suggested, the limiting null distribution of which is χ_2^2 when either κ or n, the sample size, goes to inf. Tests based on the eigenvalue of the sample cross-product matrix are also considered. Numerical examples are presented in Rivest (1986).

We tested the Hypothesis test for von Mises–Fisher distribution over Kent distribution for crater data set. The null hypothesis is whether a von Mises–Fisher distribution fits the data well, whereas the alternative is that the Kent distribution is more suitable. The details of the hypothesis testing with the *p*-value are given in Table 10.

We tested the same hypothesis test for von Mises–Fisher distribution over Kent distribution for fireball data set. The null hypothesis is whether a von Mises–Fisher distribution fits the data well, whereas the alternative is that the Kent distribution is more suitable. The details of the hypothesis testing with the *p*-value are given in Table 11.

We tested the same hypothesis test for von Mises–Fisher distribution over Kent distribution for meteor landing data set. The null hypothesis is whether a von Mises–Fisher distribution fits the data well, whereas the alternative is that the Kent distribution is more suitable. The details of the hypothesis testing with the *p*-value are given in Table 12.

7 A SPHERICAL MIXTURE MODEL FOR MODELLING EXTRATERRESTRIAL FALL DISTRIBUTION PATTERN ON THE EARTH

We model the error using maximum entropic directional statistical distribution to model the error (Assumption 2). Formally, a mixture model corresponds to the weighted mixture distribution representing the probability distribution of observations in the overall population. The Gaussian mixture model is commonly extended to fit a vector of unknown parameters. Here, we propose a spherical mixture model for modelling meteor and fireball fall distribution pattern on the Earth,

Table 12. Hypothesis test for von Mises–Fisher distribution over Kent distribution for meteor landing data set where the p-value is 0.478 and the null hypothesis is whether a von Mises–Fisher distribution fits the data well, where the alternative is that Kent distribution is more suitable.

Test	Bootstrap p-value
18465.315	0.478

the weighted mixture components of which follow von Mises–Fisher distribution.

We define the density for directional parametric mixture distribution $p(x|\boldsymbol{\theta})$, where $\boldsymbol{\theta} = (\theta_1, \theta_2, \cdots, \theta_K)$ represent appropriate parameter set, as follows.

$$p(\boldsymbol{\theta}) = \sum_{i=1}^{K} \phi_i F(x|\theta_i), \tag{9}$$

$$\begin{array}{lll} K & = & \text{number of mix ture co components} \\ N & = & \text{number of observations} \\ \theta_{i=1\ldots K} & = & \text{parameter of distribution of observation} \\ & & \text{associated with component i} \\ \phi_{i=1\ldots K} & = & \text{mixture weight, i.e. prior probability} \\ & & \text{of a particular component i} \\ \boldsymbol{\phi} & = & K\text{-dimensional vector set } \phi_{1\ldots K}\text{; sum to 1 ,} \\ z_{i=1\ldots N} & = & \text{component of observation } i \\ x_{i=1\ldots N} & = & \text{observation } i \\ F(x|\theta) & = & \text{probability distribution of an observation,} \\ & & \text{parametrized on}\theta \\ z_{i=1\ldots N} & \sim & \text{Categorical}(\boldsymbol{\phi}) \\ x_{i=1\ldots N}|z_{i=1\ldots N} & \sim & F(x_{i=1\ldots N}|\theta_{z_i}) \end{array} \tag{10}$$

In our paper, the ith vector component is characterized by $F(x|\theta_i)$ as either von Mises–Fisher distribution with weights ϕ_i, parameter θ_i as means $\boldsymbol{\mu_i}$ and concentration matrices $\boldsymbol{\kappa_i}$, or as circular uniform.

REMARK 2. For fitting the mixture von Mises–Fisher distribution to both data sets, we take the help of R package of Hornik & Grün (2014).

In this part, we want to show if both data sets follow a von Mises–Fishers distribution. To explain this, we used the **mobMF** (Hornik & Grün 2014) R package to compute the number of k (here k is the number of partitions to be considered to get the best fit of a von Mises–Fishers distribution) for which we can fit a von Mises–Fishers distribution. We used the package for the first (fireball data set). For the decrease in BIC (Bayesian information criteria), we intuitively used 15 partitions to check and get the optimal number of partitions for which the location parameter longitude and latitude satisfy the condition of following a mixture of Fisher's von Mises distribution. The EM algorithm is used in the paper, and the output that if the algorithm converges or not is satisfied by the converses of the EM algorithm given in the detailed model description mentioned in the Supporting Information.

The detailed data set 1(fireball) is given in Table 13. This tells us that among 15 partitions, we can build or satisfy a von Mises Fisher distribution for the longitude and latitude together for three partitions of the data set because it consists of the lowest BIC score among all. The probabilities or weights for each partition are defined in the Supporting Information. The values of the α or weights(ϕ) is defined as 0.3161662, 0.2981029, and 0.3857309. Fig. 9 is the pictorial view of the 3d plot of Fireball data with density.

We used the same number of partitions for data set 2 (crater data set), and the details are given in Table 14. We get six partitions

Table 13. Table containing the BIC Score for formulae, we get that three partitions can provide a mixture of Fisher–von Mises distribution for the location parameter (longitude and latitude together). We checked 15 values of k from 1 to 10. We used the fireball data set to get this table. The probabilities or weights for each partition are defined in the Supporting Information. The values of the α or the weights(ϕ) is defined as 0.3161662, 0.2981029, and 0.385730.

K values	Bayesian information criteria
1	12.05888
2	−414.94377
3	−441.93027
4	−424.15703
5	−404.66642
6	−385.16860
7	−365.67755
8	−346.72541
9	−326.55647
10	−308.28790

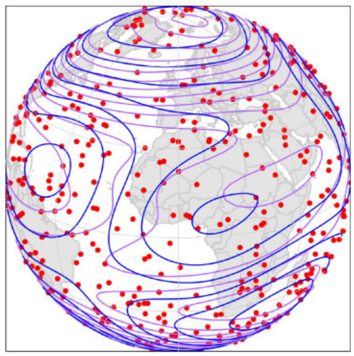

Figure 9. Spherical orthographic density plot for fireball fall on earth data set. In this picture, we used the line spacing to denote the density, and the other line defines the more prominent contour.

Table 14. Table containing the BIC score for each K value. from that, we get that six partitions can provide a mixture of Fisher–von Mises distribution for the location parameter (longitude and latitude together). We checked 10 values of k from 1 to 10. We used the crater data set to get this table. The probabilities or weights for each partition are defined in the Supporting Information. The values of the α or the weights(ϕ) are defined as 0.14895435, 0.29469552, 0.29951201, 0.15684338, 0.05714227, and 0.04285247.

K values	Bayesian information criteria
1	−14.375
2	−32.16580
3	−51.86657
4	−42.80739
5	−41.96538
6	−61.15093
7	−51.22210
8	−44.26942
9	−33.23119
10	−22.30108

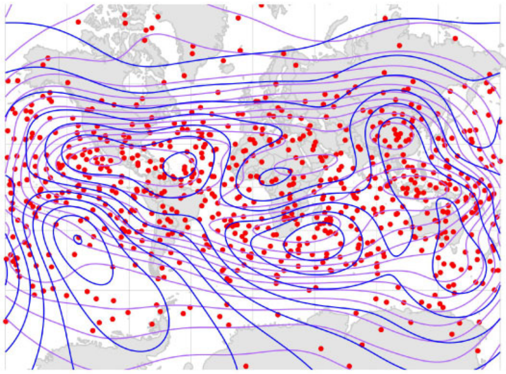

Figure 10. Spherical density estimate of fireball fall on Earth. In this picture, we used the line spacing to denote the density, and the other line defines the more prominent contour.

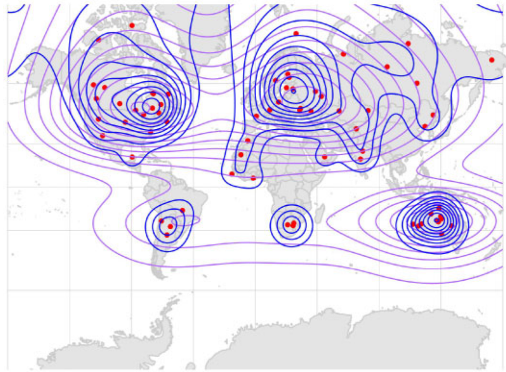

Figure 11. Spherical density estimate of crater data set on Earth. In this picture, we used the line spacing to denote the density, and other line defines the more prominent contour.

Table 15. Table containing the BIC score for each K value. From that, 13 partitions can provide a mixture of Fisher–von Mises distribution for the location parameter (longitude and latitude together). We checked 15 values of k from 1 to 15. We used the meteor landing data set to get this table. Similarly, for the created data set, we get that this will give us the weights(ϕ) or α-values as 0.091833521, 0.014696090, 0.050146550, 0.027886240, 0.009501326, 0.016462429, 0.028159021, 0.202461731, 0.055398416, 0.008716203, 0.028304857,0.091244203, and 0.375189413.

K values	Bayesian information criteria
1	−27118.06
2	−35943.30
3	−38425.78
4	−89287.07
5	−119361.45
6	−133747.85
7	−139424.86
8	−141130.45
9	−145357.52
10	−146995.48
11	−148139.44
12	−153030.39
13	−153645.05
14	−153197.94
15	−153465.51

of the second data set that can give us a von Mises–Fisher distribution for the longitude and latitude. Similarly, for the created data set, we get that this will give us the weights(ϕ) or α values as 0.14895435, 0.29469552, 0.29951201, 0.15684338, 0.05714227, and 0.04285247. Fig. 10 is the 2d plot, where we used the purple line spacing to denote the density, and the blue line defines the more prominent contour.

We used the same number of partitions for data set 3 (meteor landing data set), and the details are given in Table 15. We get six partitions of the second data set that can provide us with a von Mises–Fisher Distribution for the longitude and latitude. Similarly, for the created data set, we get that this will provide us with the weights(ϕ) or α values as 0.091833521, 0.014696090, 0.050146550, 0.027886240, 0.009501326, 0.016462429, 0.028159021, 0.202461731, 0.055398416, 0.008716203, 0.028304857, 0.091244203, and 0.375189413. Fig. 11 is the pictorial view of the 3d plot of Fireball data with density. Fig. 12 shows the Plot of both densities,

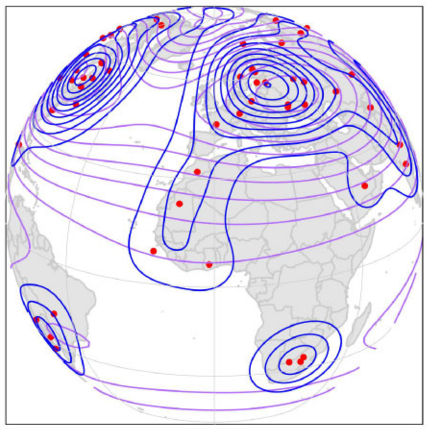

Figure 12. Spherical orthographic density plot for crater impact on Earth data set. In this picture, we used the line spacing to denote the density, and the other line defined the more prominent contour.

concerning the value of the latitude and longitude parameter.

8 DISCUSSION

(i) The first part of this paper is motivated by traditional statistical analysis in de la Fuente Marcos & de la Fuente Marcos (2015), where the B612 foundation data set was employed, and only 33 data points were observed and used traditional statistical tools, unsuitable to handle directional distributional hypothesis. Limited data set size may not provide sufficient evidence to discern clear patterns in meteor landing randomness. Hence, in this paper, we used an extensive number of data sets.

(ii) We utilized three extensive data sets as mentioned in Section 2: the craters data set, the fireball data set, shown in, and another data set, the meteor landing data set. The raw plots are Figs 1–3, respectively. We can empirically infer the existence of mixture models. None the less, we statistically proposed and validated novel directional statistical mixture models and obtained the optimal number of components using BIC.

(iii) de la Fuente Marcos & de la Fuente Marcos (2015) inferred non-randomness based on meteor fall data sets. Although our meteor landing data set is an extensive version, Fig. 3 may exemplify that the meteor landing data set is primarily obtained on land areas. It may be argued that this concentration overlooks the overall spatial distribution on Earth's surface. To address this limitation, we incorporated a total of three data sets. One data set includes fireball observations spanning the entire world map. At the same time, another encompasses crater formations caused by meteors, covering various manners and patterns of meteor landing distribution with a substantial number of data points.

(iv) In the article by de la Fuente Marcos & de la Fuente Marcos (2015), the authors evaluated spatial parameters (longitude and latitude) separately and drew conclusions regarding the distributional pattern over a sphere. However, it is essential to consider both longitude and latitude simultaneously to understand the underlying spherical distribution fully. As discussed in Section 7, we have utilized von Misses–Fisher type maximum entropic spherical distribution in this paper to address this aspect.

(v) The circular projections (latitude, longitude separately) of meteor showers, fireball showers and meteor craters on the surface of the Earth are not randomly distributed. This is somewhat expected and can be explained under the maximum entropic assumption of extraterrestrial objects falling on the Earth's surface. Using traditional statistical uniformity tests, a similar result has also been inferred in de la Fuente Marcos & de la Fuente Marcos (2015). Here, we use directional statistical tools, in contrast.

(vi) We shall inherently assume the Earth is a sphere. Based on that assumption, we may use all data sets as spherical data sets (radius of sphere scaled to unity) and show that each of the data sets of meteor showers, fireball showers, and meteor craters on the surface of the Earth are not random. They all follow a mixture of von Mises–Fisher distribution, a very popular spherical distribution. If we take latitude–longitude projection on a circle, it mostly follows von Mises (the less-dimensional version of von Mises–Fisher distribution).

(vii) We identify distinctive characteristics across the data sets: fireball falls exhibit non-uniform distribution, while meteor craters suggest evidence for uniform and von Mises distributions. Further analysis favors the von Mises distribution for crater data with the potential for further refinement. Although meteor landings deviate from a single circular distribution, we demonstrate the effectiveness of an optimal 13-mixture von Mises–Fisher distribution on a sphere for accurate modelling. Similar analyses resulted in 3 and 6 partitions for fireball and crater data sets.

9 CONCLUSIONS

In conclusion, this paper delves into the directional distribution of extraterrestrial objects impacting Earth's surface and introduces a novel directional statistical mixture model for analysing their falls, validated through meticulous examination. Contrary to the commonly accepted notion of meteoroid impacts occurring randomly, our analysis challenges this assumption. Our findings extend upon the work of de la Fuente Marcos & de la Fuente Marcos (2015), which used a small data set to conjecture the non-randomness of meteor falls on Earth's surface. The first part of this paper statistically correctly validates that using directional statistical tools on three extensive data sets on extraterrestrial objects fall on Earth's surface. The second part of this paper also discovers distinctive characteristics emerging across the data sets: fireball falls demonstrate non-uniform distribution, whereas meteor craters suggest evidence of both uniform and von Mises distributions. Further analysis leans towards favoring the von Mises distribution for crater data, with potential for refinement. Despite deviations from a single circular distribution in meteor landings, we showcase the effectiveness of an optimal 13-mixture von Mises–Fisher distribution on a sphere for accurate modelling. Similar analyses resulted in 3 and 6 partitions for fireball and crater data sets, respectively.

We have found that the location of meteor strikes does not adhere to circular uniformity pictorially give in figures in Appendix, suggesting the presence of underlying patterns and directional tendencies. The application of statistical tests, such as the Watson two-sample test, has further confirmed significant differences between parameters, rejecting the null hypothesis for both craters and fireballs.

Identifying a mixture of von Mises distribution for specific partition values underscores the complex nature of meteor fall patterns.

10 FUTURE WORKS

Overall, our study sheds light on the intricate dynamics of meteor falls and their impact locations. By recognizing underlying patterns and directional tendencies, in future we advance our understanding of these events' mechanisms, paving the way for further research into their occurrence and behaviour. From the crater data set, we get the location and the diameter of the craters created; the fireball data set consists of the location parameter, velocity and the different axis velocity, Total radiant energy, and the impact; lastly, from the meteor landing data set, we have the location and their mass. We have only used the location parameter for all data sets for the above analysis. Further, we can use the diameter, mass, velocity, and energy components integrated with the spatiotemporal features to predict the number of falls and patterns of meteors and their classification, or in a simple language, we can give a single unified model in which can expect all of this physical property of meteors.

CODE AVAILABILITY

The code about meteor landings and the data sets can be found at the following link: https://github.com/Prithwish-ghosh/Meteor-Craters.

This GitHub repository contains all the necessary code and data sets to analyse meteor landings. It is a comprehensive resource for researchers and analysts studying meteor data. The repository offers a collection of scripts and programming files that facilitate data processing, visualization, and statistical analysis.

SUPPLEMENTARY

The supplementary materials are mentioned in the Journal and the Harvard Data Verse link https://doi.org/10.7910/DVN/FLNQM5

ACKNOWLEDGEMENTS

Mr. Prithwish Ghosh and Dr. Debashis Chatterjee are thankful to Visva Bharati, Santiniketan, and NC State University Dr. Amlan Banerjee is grateful to the Indian Statistical Institute, Kolkata.

DATA AVAILABILITY

The data used for this article can be accessed through the links provided below. The fireball data sets were obtained from the NASA website and the online web sources below.

(i) The first data set, which contains information about the crater created by the meteorite landings, can be found at the following link: http://www.passc.net/EarthImpactDatabase/index.html http://www.passc.net/EarthImpactDatabase/index.html.

(ii) The second data set provides valuable fireball information and is available at: https://cneos.jpl.nasa.gov/fireballs/.

(iii) The third one, or the meteor Landing data set, is taken from https://data.nasa.gov/Space-Science/Meteorite-Landings/gh4g-9sfh.

The data set used in this paper is combined and uploaded to Harvard Dataverse https://doi.org/10.7910/DVN/FLNQM5.

REFERENCES

Ash R. B., 2012, Information Theory. Courier Corporation, Mineola, NY
Bowen E., 1956, J. Meteor, 13, 142
Brown P. et al., 1996, Meteorit. Planet. Sci., 31, 502
Brown P., Spalding R., ReVelle D. O., Tagliaferri E., Worden S., 2002, Nature, 420, 294
Bruno B. C., Fagents S., Hamilton C., Burr D., Baloga S., 2006, J. Geophys. Res.: Planets, 111
Corcoran J., Chhetri P., Stimson R., 2009, Pap. Reg. Sci., 88, 119
Dohnanyi J., 1970, J. Geophys. Res., 75, 3468
Farinella P., Vokrouhlickỳ D., Hartmann W. K., 1998, Icarus, 132, 378
Fisher D. E., Swanson M. F., 1968, J. Geophys. Res., 73, 6503
de la Fuente Marcos C., de la Fuente Marcos R., 2015, MNRAS, 446, L31
Ghosh P., A Novel Spherical Statistics-based Spatio-Temporal Analysis to Unveil Distributional Properties of Meteor Strike on Earth (unpublished doctoral dissertation), 2023, 10.13140/RG.2.2.20434.32963
Grieve R. A., 1984, J. Geophys. Res.: Solid Earth, 89, B403
Grieve R. A., Shoemaker E. M., 1994, Hazards due to Comets and Asteroids. University of Arizona Press, Tucson, AZ, p. 417
Halliday I., Griffin A. A., 1982, Meteoritics, 17, 31
Herrera V. V., Cordero G., 2016, Planet. Space Sci., 131, 111
Hochhaus S., Schoebel M., 2015, Meteor in Action. Simon and Schuster, Manhattan, NY
Hornik K., Grün B., 2014, J. Stat. Softw., 58, 1
Jammalamadaka S. R., SenGupta A., 2001, Topics in Circular Statistics. Vol. 5. World Scientific, Singapore
Jenniskens P. et al., 2021, Icarus, 365, 114469
Jupp P., 1995, New Trends Probab. Stat., 3, 123
Kronk G. W., 1988, A Descriptive Catalog. Enslow Publishers, Hillside, NJ
Kubiak T., Jonas C., 2007, Eur. J. Psychol. Assess., 23, 227
Mardia K. V., Jupp P. E., 2009, Directional Statistics. John Wiley and Sons, New York
Mardia K. V., Jupp P. E., Mardia K., 2000, Directional Statistics, Vol. 2. Wiley Online Library, New York
Millard Jr H. T., 1963, J. Geophys. Res., 68, 4297
Millard Jr H. T., Brown H., 1963, Icarus, 2, 137
Rivest L.-P., 1986, Stat. Probab. Lett., 4, 1
Robbins S. J., 2019, J. Geophys. Res.: Planets, 124, 871
Sturm S., Kenkmann T., Willmes M., Pösges G., Hiesinger H., 2015, Meteor. Planet. Sci., 50, 141
Tollenaar V., Zekollari H., Lhermitte S., Tax D. M., Debaille V., Goderis S., Claeys P., Pattyn F., 2022, Sci. Adv., 8, eabj8138
Mardia K. V., 1972, Statistics of Directional Data. Academic Press, New York
Watson G. S., 1982, J. Appl. Probab., 19, 265
Wetherill G., 1968, Science, 159, 79
Wheeler S., Watson G. S., 1964, Biometrika, 51, 256
Whillans I. M., Cassidy W., 1983, Science, 222, 55
Ye Q.-Z., Brown P. G., Pokornỳ P., 2016, MNRAS, 462, 3511
Zekollari H. et al., 2019, na

SUPPORTING INFORMATION

Supplementary data are available at *MNRAS* online.

suppl_data

Please note: Oxford University Press is not responsible for the content or functionality of any supporting materials supplied by the authors. Any queries (other than missing material) should be directed to the corresponding author for the article.

APPENDIX A:

Probability-Probability Plot for Circular Distributions

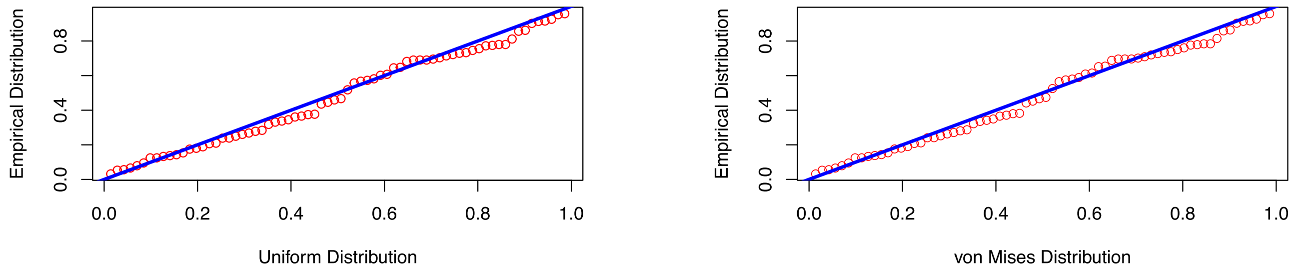

(a) Plotted Longitude probability-probability plot for crater dataset concerning circular uniform

(b) Plotted Longitude probability probability plot for crater dataset concerning vonmises

Figure A1. In this plot, we get the probability probability plot of the longitude parameter concerning both von Mises and circular uniform distribution. Here, with the naked eye, we can assume or say that the von Mises gives the better fit rather than circular uniform for the crater data set.

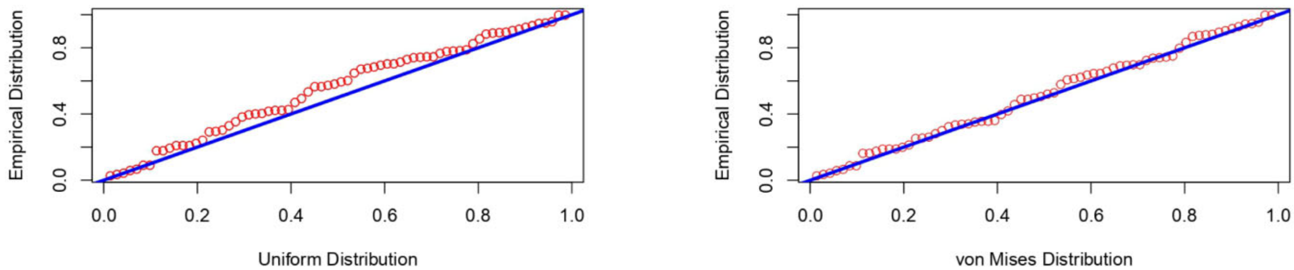

(a) Plotted the Latitude pp plot for crater Dataset concerning Circular Uniform distribution

(b) Plotted the Latitude pp plot for crater dataset concerning Vonmises Distribution

Figure A2. In this plot, we get the probability–probability plot of the latitude parameter concerning both von Mises and circular uniform distribution. Here, with the naked eye, we can assume or say that the von Mises gives the better fit rather than circular uniform for the crater data set.

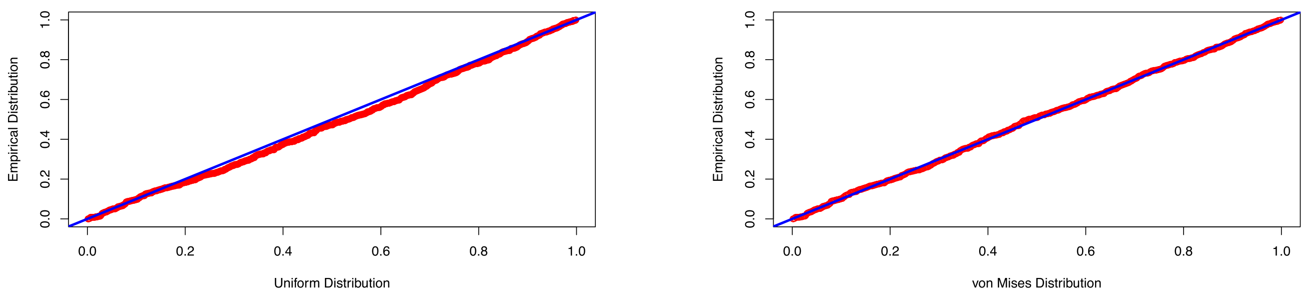

(a) Plotted the Latitude probability probability plot for fireball concerning Uniform

(b) Plotted the Latitude probability probability plot for fireball concerning Vonmises Distribution

Figure A3. In this plot, we get the probability–probability plot of the latitude parameter concerning both von Mises and circular uniform distribution. Here, with the naked eye, we can assume or say that the von Mises gives the better fit rather than the circular uniform for the fireball data set.

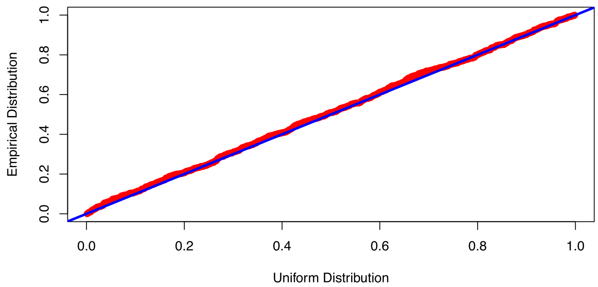

(a) For the parameter Longitude, we plotted probability Probability plot for fireball for circular Uniform

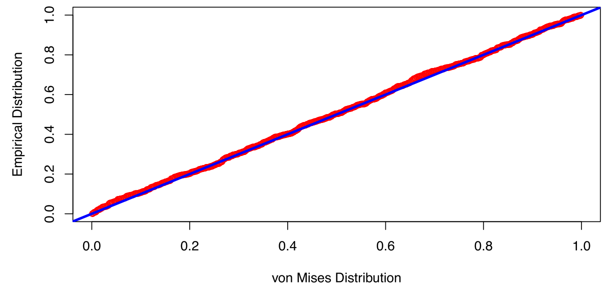

(b) For the Longitude parameter plotted the probability probability plot for fireballs for vonmises

Figure A4. In this figure, we plotted the probability probability plot for the longitude parameter of the fireball data set concerning both von Mises and circular uniform distribution. From the naked eye view, we can assume that the von Mises distribution gives a better fit than the uniform distribution.

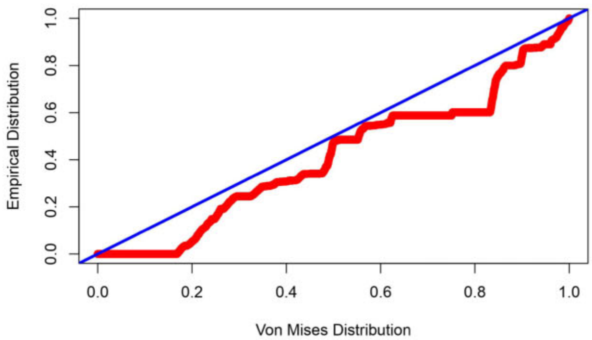

(a) Latitude probability probability plot for von Mises Distribution for Meteor Landing dataset

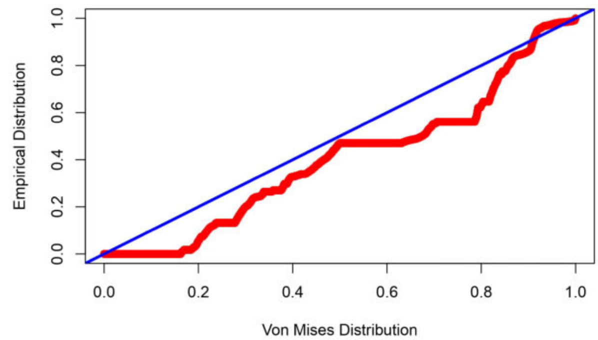

(b) Longitude probability probability plot von Mises distribution for the meteor landing Dataset

Figure A5. Plotted the location parameter's pp plot concerning von Mises distribution where we can see that the location parameters are not following von Mises distribution, a clear difference between the estimate line and the distributional plot of that two location parameter for meteor landing data set.

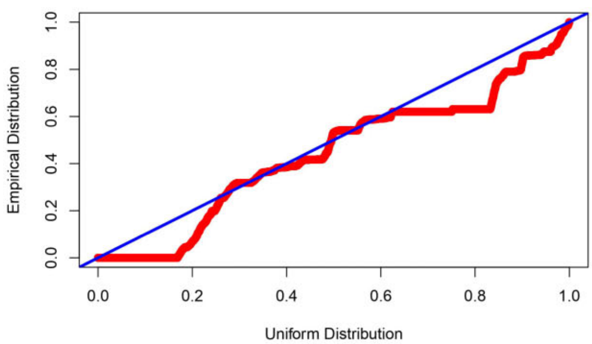

(a) Latitude probability probability plot for Circular Uniform Distribution for meteor Landing Dataset

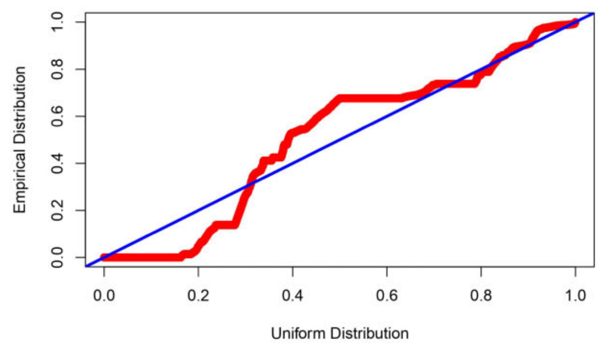

(b) Longitude probability probability plot Circular Uniform distribution for meteor Landing dataset

Figure A6. Plotted the location parameter's pp plot concerning circular uniform distribution where we can see that the location parameters are not following circular uniform distribution because of the difference between the estimate line and the distributional plot of those two location parameters for the meteor landing data set.

This paper has been typeset from a TEX/LATEX file prepared by the author.